Glutathione Transferase U13 Functions in Pathogen-Triggered Glucosinolate Metabolism[1]

Mariola Piślewska-Bednarek,[a] Ryohei Thomas Nakano,[b,c] Kei Hiruma,[b,d,2] Marta Pastorczyk,[a] Andrea Sanchez-Vallet,[e,3] Suthitar Singkaravanit-Ogawa,[d] Danuta Ciesiołka,[a] Yoshitaka Takano,[d] Antonio Molina,[e,f] Paul Schulze-Lefert,[b,c] and Paweł Bednarek[a,4]

[a]Institute of Bioorganic Chemistry, Polish Academy of Sciences, 61-704 Poznań, Poland

[b]Department of Plant Microbe Interactions, Max Planck Institute for Plant Breeding Research, 50829 Köln, Germany

[c]Cluster of Excellence on Plant Sciences (CEPLAS), Max Planck Institute for Plant Breeding Research, 50829, Köln, Germany

[d]Graduate School of Agriculture, Kyoto University, 606-8502 Kyoto, Japan

[e]Centro de Biotecnología y Genómica de Plantas, Universidad Politécnica de Madrid (UPM) - Instituto Nacional de Investigación y Tecnología Agraria y Alimentaria (INIA), 28223-Pozuelo de Alarcón (Madrid), Spain

[f]Departamento de Biotecnología-Biología Vegetal, Escuela Técnica Superior de Ingeniería Agronómica, Alimentaría y de Biosistemas, Universidad Politécnica de Madrid (UPM), 28040-Madrid, Spain

ORCID IDs: 0000-0001-5973-2300 (R.T.N.); 0000-0003-1427-1322 (Y.T.); 0000-0003-3137-7938 (A.M.); 0000-0002-3064-7775 (P.B.).

Glutathione (GSH) and indole glucosinolates (IGs) exert key functions in the immune system of the model plant Arabidopsis (*Arabidopsis thaliana*). Appropriate GSH levels are important for execution of both pre- and postinvasive disease resistance mechanisms to invasive pathogens, whereas an intact PENETRATION2 (PEN2)-pathway for IG metabolism is essential for preinvasive resistance in this species. Earlier indirect evidence suggested that the latter pathway involves conjugation of GSH with unstable products of IG metabolism and further processing of the resulting adducts to biologically active molecules. Here we describe the identification of Glutathione-*S*-Transferase class-tau member 13 (GSTU13) as an indispensable component of the PEN2 immune pathway for IG metabolism. *gstu13* mutant plants are defective in the pathogen-triggered biosynthesis of end products of the PEN2 pathway, including 4-O-β-D-glucosyl-indol-3-yl formamide, indole-3-ylmethyl amine, and raphanusamic acid. In line with this metabolic defect, lack of functional GSTU13 results in enhanced disease susceptibility toward several fungal pathogens including *Erysiphe pisi*, *Colletotrichum gloeosporioides*, and *Plectosphaerella cucumerina*. Seedlings of *gstu13* plants fail also to deposit the (1,3)-β-glucan cell wall polymer, callose, after recognition of the bacterial flg22 epitope. We show that GSTU13 mediates specifically the role of GSH in IG metabolism without noticeable impact on other immune functions of this tripeptide. We postulate that GSTU13 connects GSH with the pathogen-triggered PEN2 pathway for IG metabolism to deliver metabolites that may have numerous functions in the innate immune system of Arabidopsis.

Glutathione-*S*-transferases (GSTs) constitute a class of versatile enzymes that are ubiquitous in all living organisms and catalyze a wide range of reactions; primarily conjugation of the tripeptide glutathione (GSH) to electrophilic centers of low M_r compounds (Dixon and Edwards, 2010; Labrou et al., 2015). They are implicated in many physiological processes including xenobiotic detoxification, stress tolerance, and secondary metabolism. The latter function putatively includes the biosynthesis of unique sulfur-containing phytochemicals produced by plants belonging to the order Brassicales (Dixon et al., 2010; Bednarek, 2012a, 2012b). These compounds can be grouped into β-thioglucosides known as glucosinolates, which are present in all plant families representing this order, and sulfur-containing phytoalexins reported so far in species representing the Brassicaceae and Capparaceae plant families (Halkier and Gershenzon, 2006; Zhou et al., 2010; Pedras et al., 2011). One of the key questions related to the biosynthesis of these phytochemicals is the origin and mode of incorporation of the organic sulfur atom(s) present in their molecules. Studies on the respective biosynthetic pathways in the model plant Arabidopsis (*Arabidopsis thaliana*) indicated GSH as the sulfur donor in the biosynthesis of glucosinolates and camalexin, phytoalexin

produced in the response to microbial infection in species representing the Camelineae tribe (Bednarek et al., 2011). This biosynthetic link was inferred from the reduced accumulation of these compounds in the *phytoalexin deficient2* (*pad2*) line that is defective in GSH biosynthesis as well as from the presence of the predicted biosynthetic intermediates in the *γ-glutamyl peptidase* mutants with a malfunction in the respective biosynthetic steps downstream of GSH conjugation (Parisy et al., 2007; Schlaeppi et al., 2008; Geu-Flores et al., 2011). A contribution of GSH as sulfur donor raised the question whether GST activity is required for the biosynthesis of both compound classes. Gene coexpression and metabolic quantitative trait locus (QTL) analyses indicated GSTF9 and GSTF10 as enzymes putatively involved in the biosynthesis of Trp-derived indole glucosinolates (IGs), whereas GSTF11 and GSTU20 have been proposed to contribute to the formation of Met-derived aliphatic glucosinolates (AGs; Hirai et al., 2005; Wentzell et al., 2007). Similarly, experimental evidence suggested GSTF6 as one of GSTs contributing to camalexin biosynthesis (Su et al., 2011). However, despite these assignments it has not been unequivocally proven that formation of the respective intermediates in glucosinolate and camalexin biosynthesis requires activity of strictly defined members of the Arabidopsis GST family or that GST activity is required at all (Hirai et al., 2005; Wentzell et al., 2007; Mikkelsen et al., 2010, 2012; Su et al., 2011; Møldrup et al., 2013).

Sulfur-containing phytochemicals from Brassicales exert numerous roles in interactions with the environment, including insect deterrence and plant innate immunity (Hopkins et al., 2009; Pedras et al., 2011; Pastorczyk and Bednarek, 2016). For glucosinolates, these functions are dependent on the activity of the specialized β-thioglucoside glucohydrolases, known as myrosinases, which constitute a diverse subfamily of β-glucosidases (Nakano et al., 2017). Formed during the myrosinase-mediated glucosinolate hydrolysis, aglycones are chemically unstable and can spontaneously decompose to a number of different products including isothiocyanates (ITCs), nitriles, or thiocyanates (Wittstock et al., 2016). Experimental evidence indicates that different myrosinases can be activated in response to various stimuli and function in different physiological processes. For instance, the PENETRATION2 (PEN2) myrosinase hydrolyzes IGs in the response to attempts of pathogenic infection or recognition of microbe-associated molecular patterns (Bednarek et al., 2009; Clay et al., 2009). This reaction is critical for extracellular resistance responses against a number of filamentous plant pathogens, including *Blumeria graminis* f. sp. *hordei* (*Bgh*), *Erysiphe pisi*, *Colletotrichum gloeosporioides*, and *Plectosphaerella cucumerina* (Lipka et al., 2005; Hiruma et al., 2010; Sanchez-Vallet et al., 2010). Genetic evidence suggested that this function requires, before PEN2-catalyzed hydrolysis, CYP81F2-mediated hydroxylation at the position 4 of the indol-3-ylmethyl glucosinolate (I3G) core structure (Bednarek et al., 2009). Therefore, 4-hydroxy-I3G and 4-methoxy-I3G (4MI3G), but not I3G itself, are considered

biologically relevant substrate(s) of this myrosinase. PEN2 and CYP81F2 are also indispensable for the GLUCAN SYNTHASE-LIKE5 (GSL5)-mediated flg22 (a 22-amino acid epitope derived from bacterial flagellin)-triggered callose deposition in Arabidopsis seedlings (Jacobs et al., 2003; Nishimura et al., 2003; Clay et al., 2009). However, leaves of *pen2* plants deposited callose in response to inoculation with several fungal pathogens including *C. gloeosporioides*, *Magnaporthe oryzae*, or *Phytophthora infestans*, suggesting that penetration resistance and callose deposition are not directly linked and can be controlled by different end products of the PEN2 pathway (Lipka et al., 2005; Maeda et al., 2009; Hiruma et al., 2010).

PEN2-mediated IG hydrolysis leads to the formation of several end products including indol-3-yl methyl amine (I3A), raphanusamic acid (RA), and 4-*O*-β-ᴅ-glucosyl-indol-3-yl formamide (4OGlcI3F; Bednarek et al., 2009, 2011; Lu et al., 2015). The chemical structures of RA and I3A, combined with reduced accumulation of these metabolites in GSH-deficient plants, suggested a contribution of this tripeptide to the PEN2 pathway. It was proposed that indol-3-ylmethyl-ITC, formed after I3G hydrolysis, reacts with GSH to form a dithiocarbamate-type adduct, which is subsequently processed to I3A and RA (Fig. 1). The structure of this intermediate suggested that it could also serve as an intermediate in the biosynthesis of brassinin, the phytoalexin produced in *Brassica rapa*, and this biosynthetic link has been confirmed recently (Fig. 1; Bednarek et al., 2009; Klein and Sattely, 2017). Studies on the postingestive metabolism of glucosinolates in humans indicated that the formation of dithiocarbamate adducts in a reaction between ITCs and GSH is spontaneous, but its efficiency can be significantly enhanced by GSTs (Kolm et al., 1995; Zhang et al., 1995). However, these studies involved only aliphatic- and benzyl-ITCs. Once generated upon IG hydrolysis, indol-3-ylmethyl-ITCs are highly unstable and react easily with nucleophilic centers, even with water, by the release of a thiocyanate ion (SCN⁻; Agerbirk et al., 2009). In accordance with this reaction, the postingestive breakdown of I3G in the insect *Myzus persicae* lead to several end products including indol-3-ylmethyl-GSH, but not dithiocarbamates (Kim et al., 2008), suggesting that the capture of unstable indol-3-ylmethyl-ITCs by GSH might require efficient enzymatic catalysis mediated by a specialized GST (Fig. 1). Collectively, these findings raise questions about the identity of the GST(s) involved in IG metabolism during Arabidopsis immune responses. Candidates for such an enzyme(s) came from the studies of Wagner et al. (2002) and Dixon et al. (2009), who tested in vitro the activity of 10 and 35 Arabidopsis GSTs against six and three model substrates, respectively. According to these studies, GSTU4, GSTU5, GSTU6, GSTU13, and GSTU17 revealed highest activity against benzyl-ITC, which is routinely used as a model ITC in GST enzymatic assays. Moreover, GSTU4, GSTU6, and GSTU13 showed high specificity toward benzyl-ITC, as compared to other tested substrates, pointing to these enzymes as putative candidates for the GST(s) involved

Figure 1. Putative function of a Glutathione-S-transferase in the formation of PEN2 pathway end products. Metabolic scheme summarizing proposed involvement of GSH in the formation of different products derived from indole glucosinolates (Kim et al., 2008; Bednarek et al., 2009; Klein and Sattely, 2017).
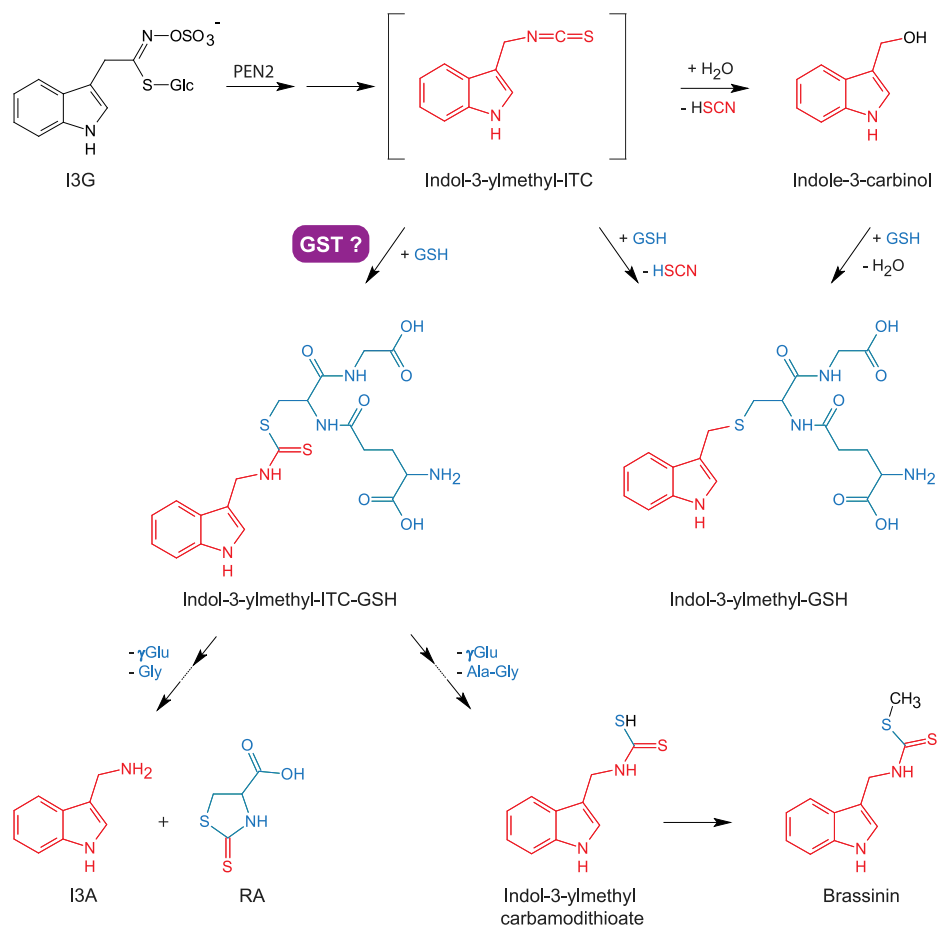
in IG metabolism during Arabidopsis immune responses (Wagner et al., 2002; Dixon et al., 2009).

In this study we identified GSTU13 as the enzyme that is essential for the proper function of the PEN2-dependent immune response pathway. Lack of functional GSTU13 in Arabidopsis *gstu13* mutants resulted not only in a deficiency of the respective metabolic end products, but also revealed *pen2*-like infection phenotypes in preinvasive defense against tested nonadapted fungal pathogens. Finally, *gstu13* plants were found to be impaired in callose deposition induced by the bacterial flg22 epitope. We postulate that GSTU13 is the enzyme that conjugates GSH with unstable indol-3-ylmethyl-ITCs formed upon PEN2-mediated IG hydrolysis, particularly in the branch of this pathway in which 4-substituted IGs are processed.

RESULTS

Coexpression Analysis Reveals GSTU13 as a Candidate GST Involved in the PEN2 Pathway

Metabolic phenotypes and entry rates of fungal pathogens observed in the GSH-deficient *cadmium sensitive2* and *pad2* lines suggested that GSH conjugation with the chemically unstable indol-3-ylmethyl-ITCs constitutes a crucial step in the pathogen-triggered IG metabolism (Fig.

1; Bednarek et al., 2009). To select a candidate GST catalyzing this putative reaction, we employed a targeted gene coexpression analysis based on 15,275 public microarray datasets (ATTED-II, v. Ath-m6.0; Nakano et al., 2017). We performed a hierarchical clustering based on genomewide and microarray-probewise Mutual Ranks (MRs; Obayashi and Kinoshita, 2009; Nakano et al., 2017) using entire Cytochrome P450 monooxygenase, β-glucosidase, and GST gene families encoded in the Arabidopsis genome (350 genes in total; Fig. 2 and Supplemental Fig. S1; Supplemental Data S1). In the gene cluster containing *PEN2* we identified *GSTU13*, besides the genes encoding the GSTs proposed for IG biosynthesis (*GSTF9* and *GSTF10*; Wentzell et al., 2007) as well as *CYP79B2/B3* and *CYP83B1* (Fig. 2). GST genes linked with AG (*GSTF11* and *GSTU20*; Hirai et al., 2005; Wentzell et al., 2007) and camalexin biosynthesis (*GSTF6*; Su et al., 2011) coclustered with those encoding the respective biosynthetic enzymes (*CYP79F1/F2* and *CYP83A1* for AG, and *CYP71A13* and *PAD3* for camalexin; Supplemental Fig. S1), indicating the existence of potential Trp-derived branch pathway-specific correlated gene expression patterns.

Interestingly, published results of in vitro enzymatic assays suggested that GSTU13 is among the Arabidopsis
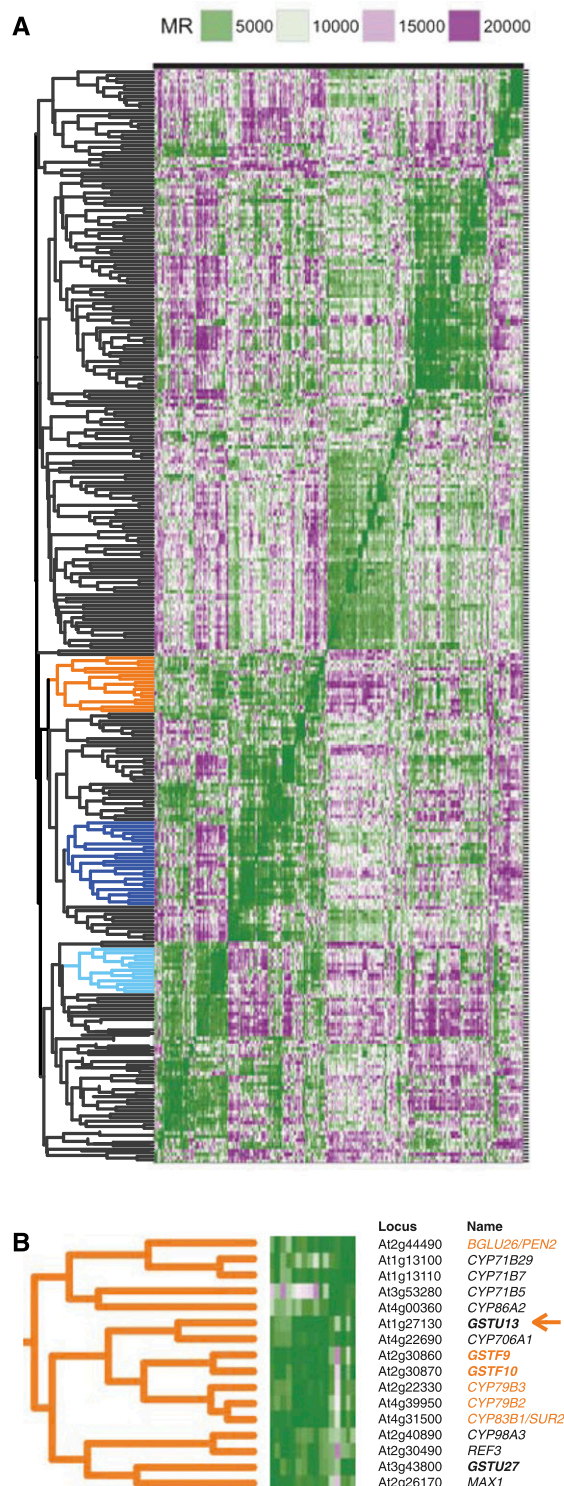
Figure 2. *GSTU13* is strongly coexpressed with *PEN2* and genes encoding indole glucosinolate-biosynthetic enzymes. A, A coexpression heatmap of *GST*s, *BGLU*s, and *CYP*s. Genes in rows and columns are aligned according to hierarchical clustering as indicated by a dendrogram. Colored clades are the clusters objectively determined for *PEN2* (orange), *CYP83A1* (blue), and *PAD3* (cyan). B, Enlarged view of the *PEN2* cluster, showing Locus IDs and gene names. *GSTs* are indicated by bold letters.

GSTs that 1) preferentially use benzyl-ITC as a substrate, and 2) have relatively high activity toward this compound compared to the other tested GSTs (Wagner et al., 2002; Dixon et al., 2009). These earlier findings, combined with our coexpression analysis, suggested a putative contribution of GSTU13 to the PEN2 pathway.

GSTU13 Contributes Differentially to the Two Branches of the Pathogen-triggered IG Metabolism

To address the assumed function of GSTU13 in IG metabolism (Fig. 2) and Arabidopsis immunity, we isolated two homozygous T-DNA insertion lines: SALK_022297 (*gstu13-1*) and SALK_050148 (*gstu13-2*). These lines carry independent insertions in the second exon of *GSTU13*, which, according to the results of our quantitative real-time PCR (qRT-PCR) analysis, compromise transcription of this gene (Supplemental Fig. S2). We inoculated these mutants, together with Col-0 and *pen2-2* plants, with conidiospores of the nonadapted powdery mildew *Bgh* and analyzed the accumulation of I3A and RA, the two metabolic products formed upon pathogen recognition from I3G in a PEN2-dependent manner. We observed significantly reduced levels of both compounds in *Bgh*-inoculated *gstu13* plants as compared to Col-0 (Fig. 3). However, accumulation of I3A and RA in *gstu13* leaves was still inducible during attempted pathogen colonization to levels that were significantly higher compared to *pen2-2* plants (Fig. 3). This suggested that GSTU13 might act in a partially redundant manner with other GST(s) in the formation of I3A and RA. We also quantified the accumulation of 4OGlcI3F, which is produced in a PEN2-dependent manner from 4MI3G or 4OHI3G upon pathogen challenge (Lu et al., 2015). We observed a strongly reduced 4OGlcI3F accumulation upon *Bgh* inoculation in plants carrying the *gstu13* mutant alleles with little, if at all, residual induction upon pathogen challenge, reminiscent of *pen2* plants (Fig. 3). This indicated that, opposite to the formation of I3A, GSTU13 is the major GST mediating pathogen-triggered 4OGlcI3F biosynthesis. Moreover, the engagement of GSTU13 in 4OGlcI3F biosynthesis suggested that the formation of this metabolite is GSH-dependent (Fig. 3). This biosynthetic link was further supported by reduced 4OGlcI3F accumulation in *Bgh*-inoculated leaves of GSH-deficient *pad2* plants (Supplemental Fig. S3)

GSTU13 Involvement in the PEN2 Pathway Is Independent from IG Biosynthesis

Besides GSH conjugation to ITCs, GST activity is also postulated to be required for IG biosynthesis per se. Metabolic QTL analysis proposed GSTF9 and GSTF10 to catalyze the respective reaction, although these assignments lack experimental validation (Wentzell et al., 2007). As the *GSTU13* expression pattern is similar to *CYP79B2*, *CYP79B3*, and *CYP83B1* (Fig. 2), we tested the possibility that GSTU13 functions in IG biosynthesis, which in turn would affect I3A, RA, and 4OGlcI3F accumulation. We analyzed IG accumulation in leaves of
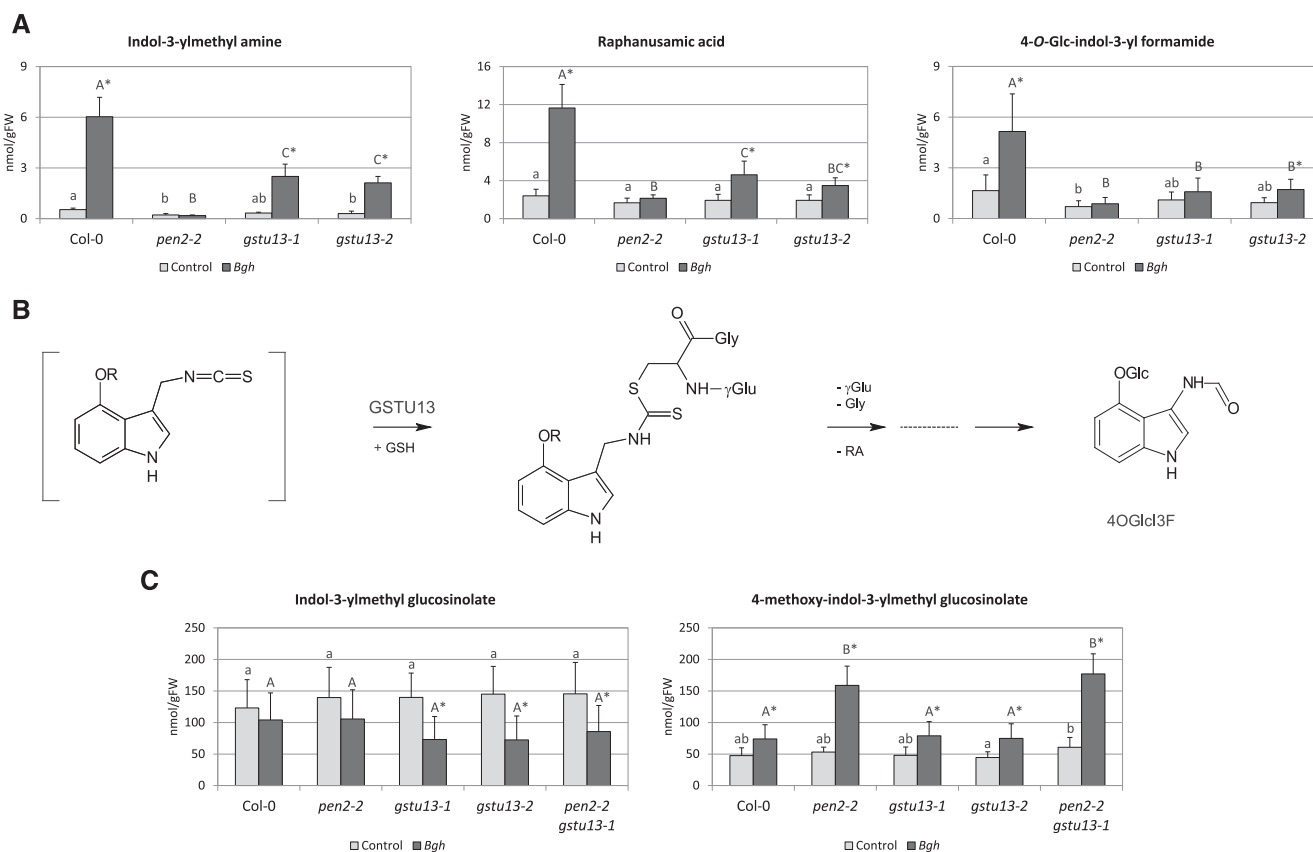
Figure 3. Metabolic phenotypes of *gstu13* mutant plants. A, Accumulation of indole glucosinolate metabolism products measured in leaves of Col-0 and indicated mutant plants 16 h after inoculation with conidiospores of the nonadapted powdery mildew *B. graminis* f. sp. *hordei*. B, Proposed involvement of GSTU13 and GSH in the formation of 4OGlcI3F. C, Indole glucosinolate accumulation in leaves of Col-0 and indicated mutant plants 16 h after inoculation with conidiospores of the nonadapted powdery mildew *B. graminis* f. sp. *hordei*. Presented results (A and C) are means ± SD from three independent experiments with three biological replicates in each (*n* = 9). Significantly different statistical groups of genotypes indicated by the analyses of variance (ANOVA; *P* < 0.05, Bonferroni's test) are shown with lower case (control) and upper case (*Bgh*) letters. Values marked with asterisks are significantly different from respective controls (Student's *t*-test; *P* < 0.01). FW, fresh weight.

naïve and *Bgh*-inoculated *gstu13* single and *pen2-2 gstu13-1* double knockouts and found that *gstu13* plants accumulated wild-type levels of I3G and 4MI3G. Moreover, *pen2 gstu13* double knockout plants produced elevated amounts of 4MI3G in response to pathogen inoculation, similar to *pen2-2* mutant plants (Fig. 3). These results clearly indicate that the requirement of GSTU13 for I3A, RA, and 4OGlcI3F formation does not result from its contribution to IG biosynthesis, but rather from its function in IG metabolism, downstream of PEN2 myrosinase (Fig. 1).

The PEN2 Pathway for Preinvasive Disease Resistance Is Dependent on GSTU13 Activity

To examine whether the defects in IG metabolism observed in *gstu13* plants result in altered infection phenotypes upon pathogen inoculation, we determined fungal entry rates of the nonadapted powdery mildew *E. pisi* on the aforementioned collection of Arabidopsis mutants. Our analysis revealed a *pen2*-like defect in preinvasive resistance of both tested *gstu13* mutant lines (Fig. 4). We also inoculated these plants with a nonadapted hemibiotrophic pathogen, *C. gloeosporioides*, which revealed comparable elevated fungal entry rates on *gstu13* and *pen2-2* plants (Fig. 4A). It has been reported that in the presence of Glc, *C. gloeosporioides* penetrates epidermal cells of *pen2* leaves using an unusual hyphal tip entry mode (Hiruma et al., 2010). Our microscopic analysis of plant-fungus contact sites showed that the same entry mode is utilized by *C. gloeosporioides* when penetrating into leaf epidermal cells of *gstu13* plants (Fig. 4). Overall, the experiments with *E. pisi* and *C. gloeosporioides* indicated that the defects in preinvasive resistance of *pen2-2* and *gstu13* lines are indistinguishable. In addition, the entry rates of both pathogenic fungi on *pen2-2 gstu13-1* double mutant plants did not differ significantly from those observed for *pen2-2* and *gstu13* single mutants (Fig. 4), indicating that GSTU13 and PEN2 act in the same preinvasive resistance pathway.
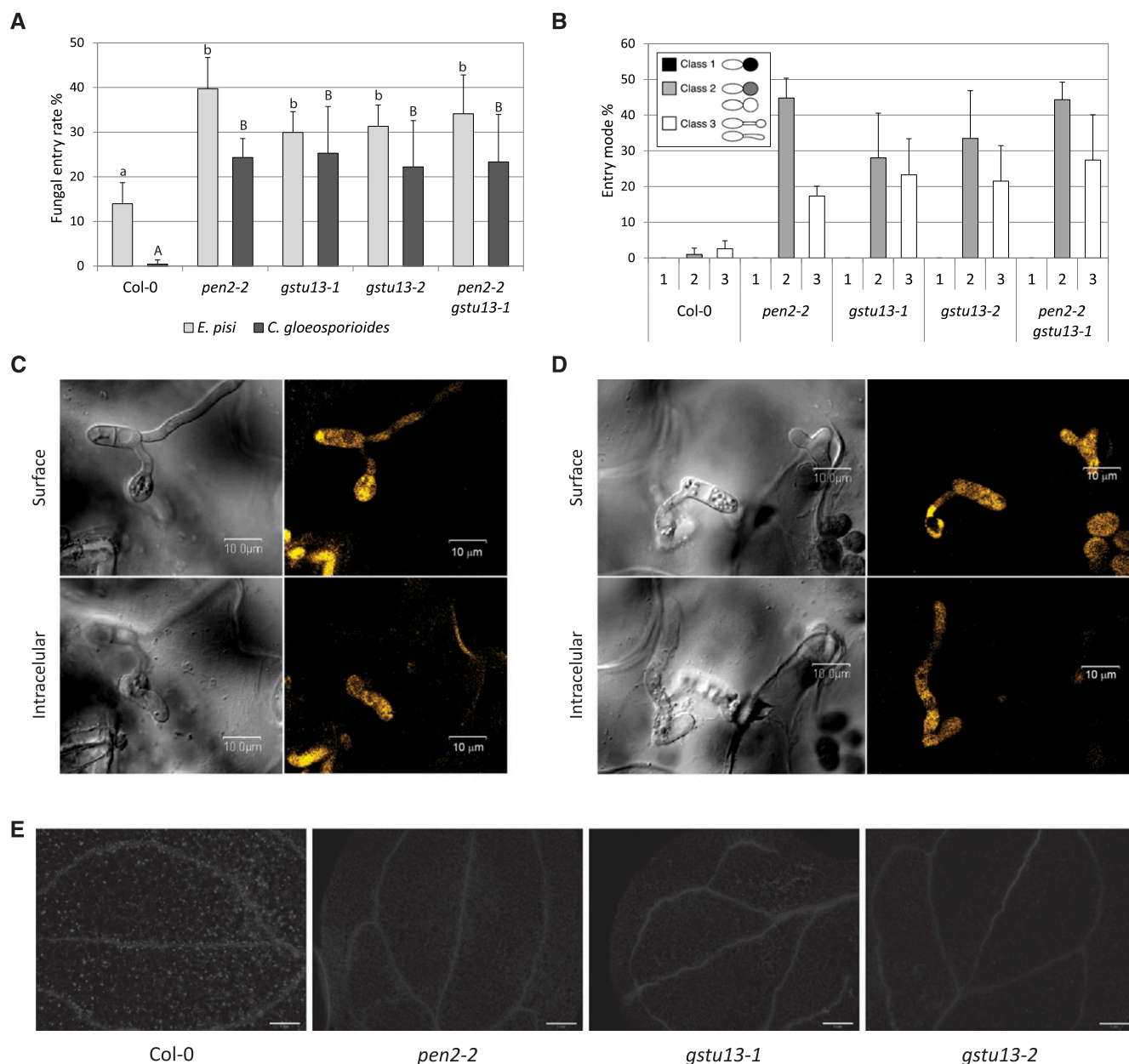
Figure 4. GSTU13 is essential for proper immune responses in Arabidopsis. A, Frequency of invasive growth at *E. pisi* and *C. gloeosporioides* interaction sites on Arabidopsis genotypes scored 48 and 14 h, respectively, after inoculation with conidiospores. Presented results are means ± SD from three independent experiments. Significantly different statistical groups of genotypes indicated by ANOVA ($P < 0.05$, Bonferroni's test) are shown with lower case (*E. pisi*) and upper case (*C. gloeosporioides*) letters. B, Invasion manner of *C. gloeosporioides* into epidermal cells of indicated mutants. Class 1, melanized appressorium; class 2, nonmelanized appressorium; class 3, hyphal tip entry. The percentage of successful invasion by each class structure was based on the total number of each class structure. The means and SDs were calculated from three independent experiments. C and D, Formation of invasive hyphae by aberrant fungal structures. Conidia of *C. gloeosporioides* expressing GFP were inoculated on the *gstu13-1* mutant, and inoculated plants were incubated for 14 h. C, Invasion via nonmelanized appressorium (class 2). D, Invasion via a tiny swollen structure (class 3). Bars = 10 μm. E, *gstu13* mutations suppress flg22-dependent callose deposition. 10-d-old seedlings were treated with flg22 for 24 h and subjected to callose staining. Bars = 1 mm.

GSTU13 Is Essential for flg22-triggered Callose Deposition in Arabidopsis Seedlings

PEN2-mediated metabolism of 4-substituted IGs has been also reported to be required for the GSL5/PMR4-mediated callose deposition in Arabidopsis seedlings in response to application of the bacterial flg22 epitope, a microbe-associated molecular pattern that is perceived by the Flagellin Sensing 2 immune receptor (Clay et al., 2009). However, retained deposition of this cell-wall-associated

β-glucan polymer observed in pathogen-inoculated leaves of adult *pen2* plants suggested that penetration resistance and callose deposition could be controlled by different end products of the PEN2/CYP81F2 pathway (Bednarek, 2012a, 2012b). To test if GSTU13 also contributes to the formation of the IG-derived product(s) required for callose deposition, we analyzed this response in 10-d-old *gstu13* seedlings. Aniline Blue staining revealed that, similar to the *pen2-2* mutant, flg22-induced callose deposition was strongly abrogated in the *gstu13* seedlings (Fig. 4). This result indicated that GSTU13 is indispensable not only for preinvasive resistance, but also for the flg22-induced callose deposition. Overall, this suggests a tight functional link between GSTU13 and PEN2 in cotyledons and adult leaves and in response to both fungal and bacterial triggers of plant innate immune responses.

Specific Role of GSTU13 in Preinvasive But Not Postinvasive Disease Resistance

Apart from a function in preinvasive disease resistance, GSH acts also in postinvasive immune responses to hemibiotrophic and necrotrophic pathogens, as evidenced by sustained hyphal growth inside *pad2* mutant leaves (Fig. 5), which is independent of the PEN2 pathway (Sanchez-Vallet et al., 2010; Hiruma et al., 2013). We dissected the functional relations among GSTU13, GSH, and PEN2 by testing the potential contribution of GSTU13 to postinvasive immunity. When *gstu13* mutants were inoculated with a suspension of *C. gloeosporioides* conidia, the necrotic lesions on *gstu13* leaves did not spread beyond the margins of leaf-inoculated conidia droplets (Fig. 5). Microscopic analysis of plant-pathogen contact sites of leaves of this genotype confirmed a containment of fungal hyphae inside the first penetrated epidermal cells (Fig. 5). In addition, when *gstu13* leaves were inoculated with a suspension of *P. cucumerina* conidia, the fungal biomass was indistinguishable between *pen2-2* and *gstu13* single mutant plants (Fig. 5). Consistent with this, *gstu13* mutants did not reveal any defects in the *P. cucumerina*-triggered
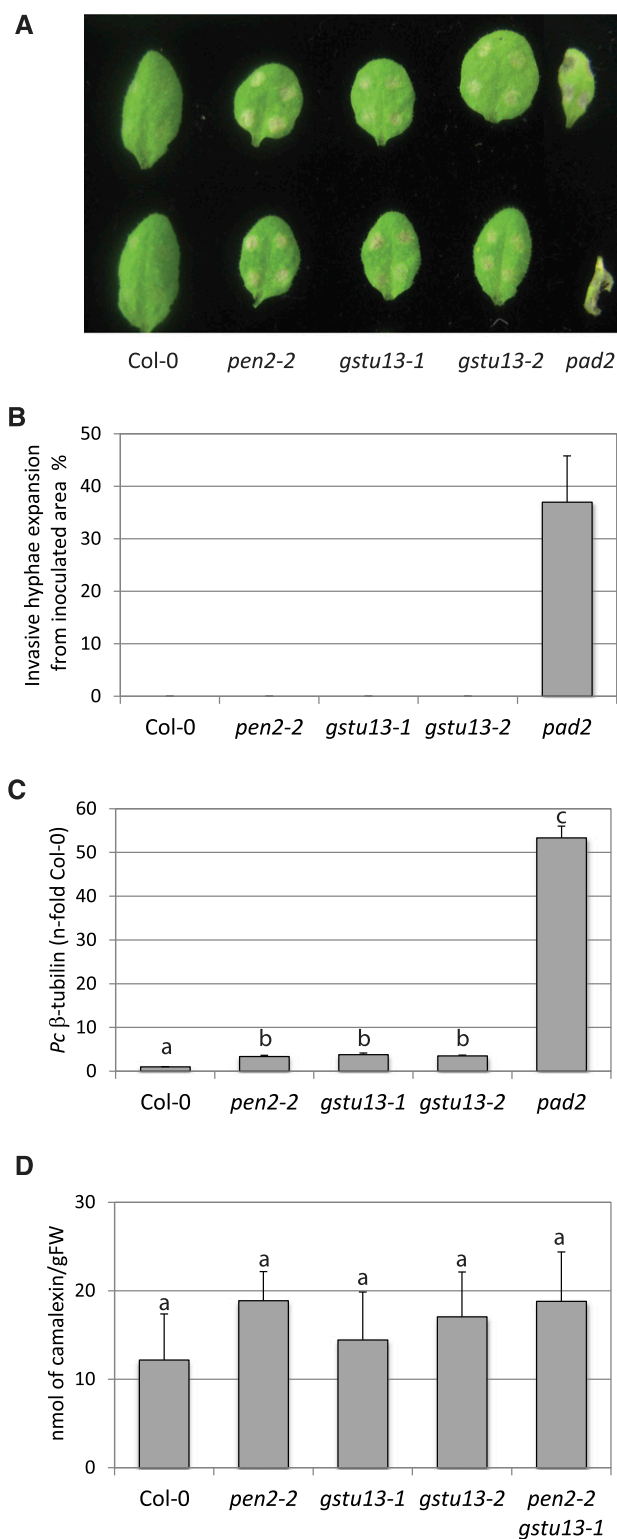
Figure 5. Opposite to glutathione GSTU13 is dispensable for post-invasive immune responses. A, Lesions induced by *C. gloeosporioides*. Conidia of *C. gloeosporioides* were drop-inoculated onto leaves of indicated genotypes (4 week old), and the inoculated plants were incubated for 6 d. Only in leaves of the glutathione-deficient *pad2* plants, lesions expanded from the inoculated areas. B, *C. gloeosporioides* hyphal extension from the inoculated areas. At 4 dpi, inoculated leaves were stained with Trypan Blue and used to determine the expansion rate of invasive necrotrophic hyphae from the inoculated area by light microscopy. The means and sds were calculated from three independent experiments. C, Real-time PCR quantification of *P. cucumerina* DNA (*Pc* β-tubilin) in leaves of inoculated plants at 5 dpi. Values (sds) are represented as the average of the *n*-fold fungal DNA levels, relative to the wild-type (Col-0) plants. Letters indicate significantly different statistical groups of genotypes (ANOVA; $P < 0.05$, Bonferroni's test). D, Camalexin accumulation in leaves of Col-0 and indicated mutant plants 48 h after inoculation with conidiospores of the adapted strain of *P. cucumerina*. Presented results are means ± sd from two independent experiments with four biological replicates in each ($n = 8$). Letters indicate significantly different statistical groups of genotypes (ANOVA; $P < 0.05$, Bonferroni's test).

accumulation of camalexin, which was shown to have a function in postinvasive resistance (Fig. 5). These findings indicated that GSTU13 is dispensable for postinvasive immunity and utilizes GSH substrate exclusively for PEN2-dependent preinvasive immune responses. Overall, our results clearly demonstrated that GSTU13 works together with PEN2 to confer preinvasive immunity against a wide range of non-adapted fungal pathogens.

GSTU13 Deficiency Does Not Affect Accumulation of Indole-3-Carboxylic Acids

A recent report indicated that IGs and PEN2 myrosinase are indispensable for the induced accumulation of indole-3-carboxylic acid (I3CA) derivatives upon flg22 treatment (Frerigmann et al., 2016). To test whether this also requires GSTU13 activity, we monitored the accumulation of I3CAGlc and 6OGlcI3CA in leaves of *gstu13* plants upon spray application of flg22 epitope. Our analysis revealed that, opposite to *pen2-2* plants, *gstu13* plants accumulated wild-type-like levels of both I3CA derivatives (Fig. 6). Similarly, the *cyp81F2-1* knockout line retained the capacity for the accumulation of I3CAs (Fig. 6), indicating that flg22-triggered accumulation of I3CAs correlates with the levels of I3G metabolism products rather than metabolites derived from the hydrolysis of 4-substituted IGs. In accordance with this notion and similar to *Bgh*-inoculated plants, we observed intermediate levels of I3A and RA in the flg22-treated *gstu13* plants as compared to wild-type Col-0 and *pen2-2* plants (Supplemental Fig. S4). Collectively, this suggests that the contribution of yet unknown GST(s) to the formation of I3G-derived metabolites is sufficient to trigger I3CA accumulation (Fig. 6). Alternatively, this function of the PEN2 pathway might be uncoupled from GSH and GST activity.

GSTU13 Represents a Brassicaceae-specific Innovation in the GST Family

Our results indicated that a particular isoform of the GST family is required for proper IG metabolism and preinvasive disease resistance in Arabidopsis. This raised the question whether *At*GSTU13 represents a GSTU subclade that evolved specifically in the Brassicaceae to act in the PEN2 pathway, which is conserved in this plant family (Bednarek et al., 2011). We collected nucleic acid sequences of GSTs encoded in a wide range of plant genomes, including green algae, and analyzed their phylogenetic relationship (Fig. 7 and Supplemental Fig. S5). The maximum-likelihood (ML) tree shown in Figure 7 illustrates that *GSTU13* belonged to a subclade composed of *GSTU11-18*. Within this clade, *GSTU15-18* formed a monophyletic group with *GSTUs* from non-Brassicaceae plants, whereas *GSTU11-14* members were exclusively found in species belonging to Brassicaceae (Fig. 7). This supports our idea that *GSTU13* is a

part of a lineage-specific functional module for immune responses defined by the metabolic cascade comprising PEN2, CYP81F2, and other enzymes. Finally, we asked whether *GSTU13* is also conserved in the genus *Capsella*, in which the PEN2 pathway is functionally inactive (Bednarek et al., 2011). Unexpectedly, *Capsella rubella* and *Capsella grandiflora* both encode *GSTs* showing highest similarity to Arabidopsis *GSTU13*, *GSTU14*, and *GSTU11* (Fig. 7), but not those to Arabidopsis *GSTU12*. This suggests an additional role(s) of *GSTU13/14* isoforms in Brassicaceae that is maintained in the genus *Capsella* or that the function of *GSTU13/14* in this genus is allocated to *GSTU12*, perhaps via a functional redundancy among these isoforms. Irrespective of this complication and in clear contrast to *GSTU15-18*, *GSTU11-14* members represent a Brassicaceae-specific innovation of GSTs that was necessary for the evolution of a lineage-restricted functional module for preinvasive immunity.

DISCUSSION

GSTU13 Is Strictly Necessary for the Immune Function of IGs in Arabidopsis Leaves

Chemical structures of RA and I3A, combined with a dependency of their formation on GSH supply, suggested indol-3-ylmethyl-ITC-GSH conjugates as intermediates in pathogen-triggered IG metabolism in Brassicaceae (Fig. 1; Bednarek et al., 2009). A possible formation of such conjugates in planta was further supported by the identification of indolyl-dithiocarbamate glucoside during engineering of brassinin biosynthesis in *Nicotiana benthamiana* (Klein and Sattely, 2017). Here we identified GSTU13 as the enzyme involved in the pathogen- and flg22-triggered formation of RA and I3A, which suggests that it catalyzes in planta conjugation of indol-3-ylmethyl-ITCs with GSH. Consistent with our findings, GSTU13 was among few Arabidopsis GSTs that exhibited a relatively high activity and preference against benzyl-ITC over other substrates during in vitro enzymatic assays (Wagner et al., 2002; Dixon et al., 2009). Only GSTU4, GSTU5, GSTU6, and GSTU17 converted benzyl-ITC with similar rates as GSTU13, among which only GSTU4, GSTU6, and GSTU13 showed specificity toward this particular substrate. These earlier findings support the putative function of GSTU13 in conjugating GSH to indol-3-ylmethytl-ITC.

Besides the involvement in I3A and RA formation, our analysis revealed a striking requirement of GSTU13 for 4OGlcI3F biosynthesis upon pathogen recognition and immune response activation (Fig. 3). This finding, combined with reduced 4OGlcI3F accumulation levels in leaves of GSH-deficient plants, indicated that this product is derived from the respective dithiocarbamate-type intermediate formed in a GSTU13-dependent manner upon PEN2-mediated hydrolysis of 4MI3G or 4OHI3G (Fig. 3). In addition, the phenotypes observed in *gstu13* mutants upon pathogen inoculation or flg22

Figure 6. GSTU13, unlike PEN2, is not required for flg22-triggered accumulation of indole-3-carboxylic acids. A, Accumulation of indole-3-carboxylic acids measured in leaves of Col-0 and indicated mutant plants 24 h after treatment with the bacterial flagellin epitope flg22. Presented results are means ± SD from three independent experiments with four biological replicates in each ($n = 12$). Significantly different statistical groups of genotypes indicated by ANOVA ($P < 0.05$, Bonferroni's test) are shown with lowercase (control) and upper-case (flg22) letters. B, GSTU13 contributes differentially to the two branches of PEN2 pathway. GSTU13 is the major GST involved in the pathogen-triggered conversion of 4MI3G to 4OGlcI3F. Consequently, GSTU13 is indispensable for preinvasive resistance against fungal pathogens and flg22-iduced callose deposition. Metabolism of I3G is additionally mediated by an unidentified GST, which is involved in the formation of I3A and RA. This in turn, likely contributes to the induction of I3CA biosynthesis. Alternatively, induction of I3CA biosynthesis could be completely independent from GST activity. FW, fresh weight.
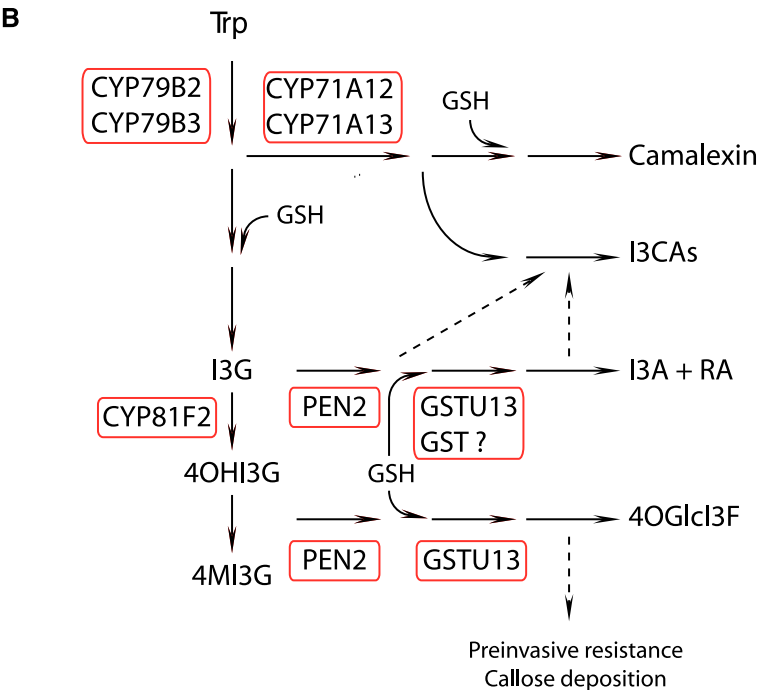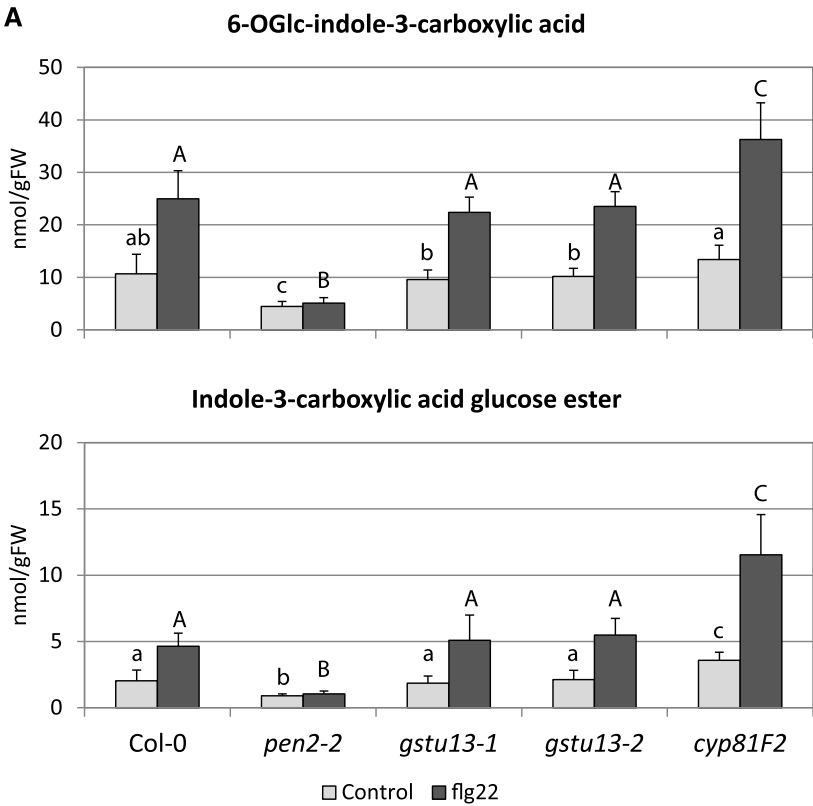
treatment revealed that this contribution of GSTU13 to the pathogen-triggered metabolism of 4-substituted IGs is indispensable for the proper function of the PEN2 immune pathway, including preinvasive disease resistance and callose deposition (Fig. 4). Our findings indicated that GSTU13 is not involved in other biosynthetic pathways, including IG and camalexin formation (Figs. 3 and 5), nor in a GSH function for postinvasive immunity against necrotrophic and hemibiotrophic fungal pathogens (Fig. 5).
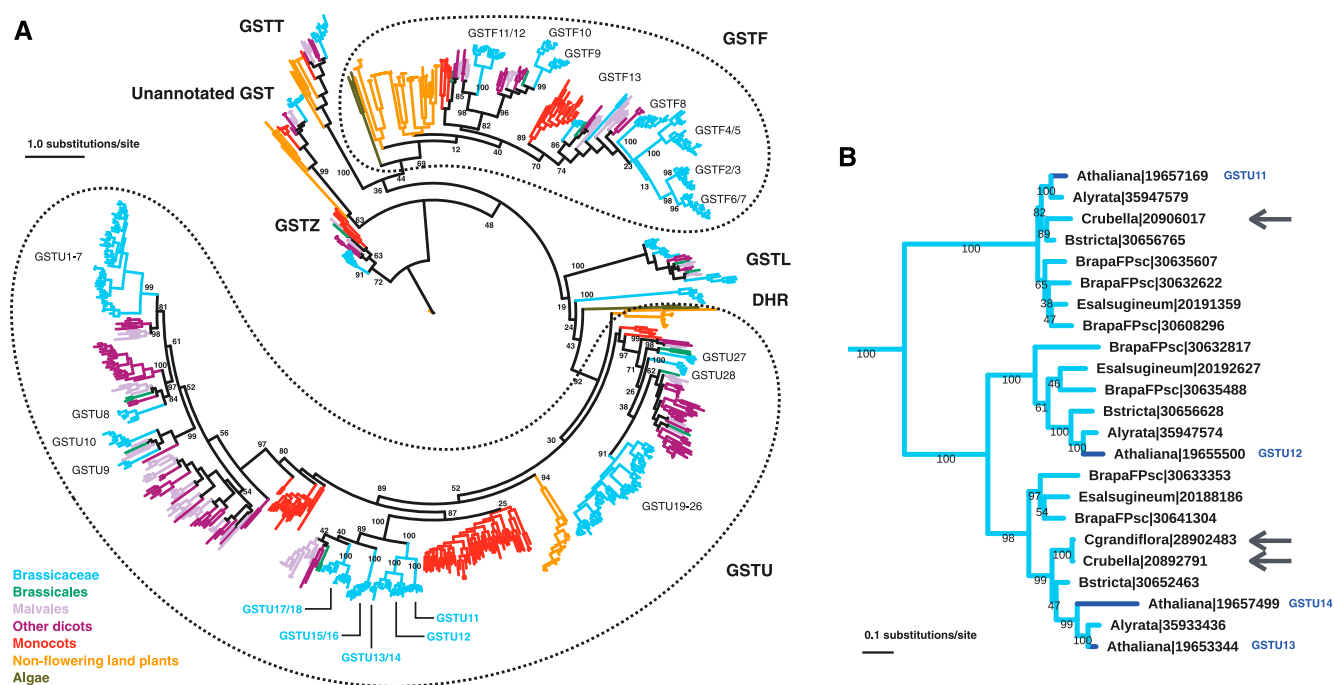
Figure 7. *GSTU13*, together with *GSTU11*, *GSTU12*, and *GSTU14*, forms a Brassicaceae-specific GST subfamily. A, An ML tree of GSTs encoded on a wide range of plant genome sequences. Colored nodes indicate a node specific to Brassicaceae (cyan), a basal Brassicales *Carica papaya* (green), Malvales (light purple), other dicotyledonous plants (purple), monocotyledonous plants (red), nonflowering land plants (a lycophyte and bryophytes; orange), and green algae (dark yellow). GST families are indicated by bold letters and some representative Arabidopsis isoforms of GSTU and GSTF subfamilies are indicated by plain letters. Only key bootstrap values from 100 replicates are indicated. The identical tree with all bootstrap values and gene names can be found in Supplemental Figure S6. B, An enlarged view of GSTU11-14 subclade. Genes from Arabidopsis are indicated by blue nodes. Black arrows indicate isoforms identified from the *Capsella* genus. Gene names are shown with species names and PAC transcript IDs. A corresponding gene table can be found in Supplemental Data S2.

Is GST-mediated GSH Conjugation Rare in the Biosynthesis of Plant Secondary Metabolites?

Although GSTs are postulated to function in plant primary and secondary metabolism, in addition to many other roles such as redox regulation, genetic evidence for such a contribution has been proven only for a few representatives of this enzyme class (Dixon et al., 2010). Moreover, the confirmed functions are frequently not necessarily linked with GST catalytic activity. For instance, BRONZE2, ANTHOCYANIN9, and TRANSPARENT TESTA19 GSTs from maize (*Zea mays*), petunia, and Arabidopsis, respectively, are required for proper sequestration of anthocyanins into the vacuole without GSH conjugation being involved (Marrs et al., 1995; Alfenito et al., 1998; Kitamura et al., 2004). Experimental evidence suggests that these GSTs cotransport anthocyanins together with GSH that is required to facilitate vacuolar import of anthocyanins by respective ATP-Binding Cassette transporters (Mueller et al., 2000; Sun et al., 2012; Francisco et al., 2013). Likewise, GSH conjugates and their derivatives have been so far only identified as biosynthetic intermediates of glucosinolate, camalexin, and brassinin (Böttcher et al., 2009; Geu-Flores et al., 2011; Klein and

Sattely, 2017). This suggests that GST-mediated conjugation of GSH is rather rare in plant secondary metabolism and possibly unique for plant species producing sulfur-containing secondary metabolites.

Specialized GSTs in the Biosynthesis of Sulfur-containing Metabolites in Brassicales

The observed indispensability of GSTU13 for the proper metabolism of IGs during immune responses is in marked contrast to findings on GSTs that are putatively involved in glucosinolate biosynthesis, but whose function has not been supported by mutant phenotypes. Moreover, metabolic engineering of glucoraphanin (AG) biosynthesis in *N. benthamiana* and I3G biosynthesis in *Saccharomyces cerevisiae* indicated that the expression of GSTF9 or GSTF11 may eventually increase glucosinolate accumulation levels, but this is not essential for their production (Mikkelsen et al., 2010, 2012). Similarly, although the *gstf6* mutant has been shown to be partially deficient (approximately 20% reduction, as compared to the wild-type plants) in camalexin production in response to *Botrytis cinerea* (Su et al., 2011), the efficiency of camalexin biosynthesis

engineering in *N. benthamiana* was not dependent on the presence of *At*GSTF6 (Møldrup et al., 2013). These findings suggested that nonspecific endogenous GSTs from other organisms can efficiently catalyze the respective steps in glucosinolate and camalexin biosynthesis. Alternatively, it remains plausible that the respective reactions are spontaneous, and their efficiency can be only moderately, if at all, improved by the presence of specialized GSTs. In contrast, unlike the GSH acceptors in glucosinolate and camalexin biosynthesis, the chemical instability of indol-3-ylmethyl-ITCs rather excludes a spontaneous formation of the corresponding dithiocarbamate-type adducts (Fig. 1; Kim et al., 2008; Agerbirk et al., 2009). Moreover, significant amounts of indole-3-carbinol, generated upon transient expression of brassinin biosynthetic enzymes in *N. benthamiana*, suggested that although nonspecialized GSTs from other species might support the formation of the dithiocarbamate-type adducts from indol-3-ylmethyl-ITCs, they are not efficient enough to prevent the release of undesired side products (Fig. 1; Klein and Sattely, 2017). Collectively, these findings suggest that specialized GSTs cannot be excluded for glucosinolate and camalexin biosynthesis, and that these enzymes are indispensable for efficient function of the PEN2 pathway and brassinin biosynthesis.

At present it is not clear whether the specific contribution of GSTU13 to the PEN2 pathway results predominantly from its substrate specificity, as suggested by in vitro studies of Wagner et al. (2002) and Dixon et al. (2009), or additionally from other factors such as a unique subcellular localization. PEN2 is associated with peroxisomal and mitochondrial membranes, and its function in immunity is dependent on the relocalization of mitochondria to sites of attempted pathogen entry (Lipka et al., 2005; Fuchs et al., 2016). This suggests that the metabolic processes responsible for preinvasive disease resistance occur directly underneath pathogen contact sites. Therefore, it is plausible that GSTU13 is also remobilized to these sites upon pathogen challenge.

Functional Differentiation among Closely Related GSTU11-14 Isoforms

Unlike the formation of 4OGlcI3F, the biosynthesis of I3A and RA is only partially dependent on GSTU13 (Fig. 3). This raises the question of which additional GST contributes to this branch of IG metabolism. Our phylogenomic analysis suggested that GSTU13, together with GSTU11, GSTU12, and GSTU14, evolved in Brassicaceae to function in metabolic processes unique for this plant family (Fig. 7). However, GSTU11, GSTU12, and GSTU14 are almost exclusively expressed in roots (Dixon et al., 2010), which makes their putative contribution to the formation of RA and I3A in the *gstu13* mutant leaves rather unlikely. Moreover, GSTU14 lacks the conserved Ser residue, which is considered critical for GSH binding, and its catalytic activity remains to be

proven (Dixon et al., 2009; Krajewski et al., 2013). Heterologously expressed GSTU11 was not active toward benzyl-ITC, whereas GSTU12 was shown to localize to the nucleus, a different subcellular compartment compared to mitochondria- and peroxisome-associated PEN2 (Dixon et al., 2009; Fuchs et al., 2016). Thus, it remains unclear which GST(s) are responsible for the residual I3A and RA biosynthesis in the *gstu13* mutant background.

Peptidases in Pathogen-triggered IG Metabolism

To generate I3A and RA from I3G and 4OGlcI3F from 4OH- or 4MI3G, our model predicts two types of peptidases that cleave γ-Glu and Gly residues from indol-3-ylmethyl-ITC-GSH (Figs. 1 and 3). In glucosinolate and camalexin biosynthesis, γ-Glutamyl Peptidase1 (GGP1) and GGP3 have been identified as redundant enzymes that remove γ-Glu from the corresponding GSH conjugates (Geu-Flores et al., 2011). As indicated by transient gene expression in *N. benthamiana*, at least one of these GGPs could be also involved in brassinin biosynthesis in *B. rapa* (Klein and Sattely, 2017). The carboxypeptidase(s) cleaving Gly in glucosinolate or phytoalexin biosynthesis so far has not been identified. However, in the case of glucosinolate and brassinin pathways, this step seems to be not essential, as the subsequent enzyme, SUPERROOT1 C-*S* lyase, can efficiently metabolize biosynthetic intermediates with retained Gly (Geu-Flores et al., 2011). The peptidase(s) removing γ-Glu from indol-3-ylmethyl-ITC-GSH has not been reported, but PHYTOCHELATIN SYNTHASE1 has been proposed as the carboxypeptidase that may contribute to the PEN2 pathway (Clay et al., 2009; Kühnlenz et al., 2015). This suggests that *gstu13* and *pcs1* mutant plants may serve together as an important future tool to develop a targeted metabolic profiling protocol for the characterization of the deduced biosynthetic intermediates of the PEN2 pathway.

MATERIALS AND METHODS

Plant Material

Seeds of *gstu13* lines T-DNA lines, SALK_022297 (*gstu13-1*) and SALK_050148 (*gstu13-2*), have been obtained from the Nottingham Arabidopsis Stock Center (stocks N522297 and N550148, respectively). Oligonucleotide sequences used for isolation of homozygous mutants were: 5′-CACTCATGCA-TAGCGAAGAGG-3′ (LP; *gstu13-1*), 5′-GATCCGATTTACGGATATGGG-3′ (RP; *gstu13-1*), 5′-CGTTCCTTCAATCCTTCCTTC-3′ (LP; *gstu13-2*), 5′-GAAAGGT-GAGGTTTCCTCCAG-3′ (RP; *gstu13-2*), and 5′-TGGTTCACGTAGTGGGCCATCG-3′ (LBa1 SALK primer). *GSTU13* expression levels in leaves of the obtained homozygous lines have been checked with qRT-PCR using the protocol described earlier (Frerigmann et al., 2016) and normalized to *ACTIN2*. Primer sequences were as follows: 5′-TTTTGGGCTCAGTACATCGA-3′ (LP, *GSTU13*), 5′-ATTCG-CAAAGCAAAAGTTCAA-3′ (RP, *GSTU13*), 5′-CCGGTATTGTGCTGGATTCT-3′ (LP, *ACTIN2*), and 5′-AATTTCCCGCTCTGCTGTTG-3′ (RP, *ACTIN2*). The *pen2-2*, *cyp81F2-1*, and *pad2* lines have been reported earlier (Bednarek et al., 2009). The *pen2-2 gstu13-1* double knockout plants have been generated by crosses of the respective single mutants. For inoculations with powdery mildews, flg22 spray-inoculation plants were grown in growth chambers at 20°C to 23°C with a 10-h photoperiod and a light intensity of approximately 150 μE m^{-2} s^{-1} for 4 weeks.

HPLC Analysis of Secondary Metabolites

Four-week-old plants of selected genotypes were inoculated with *Blumeria graminis* f. sp *hordei* (isolate K1) using a settling tower (Lipka et al., 2005), spray-inoculated with *Plectospaerella cucumerina* (isolate BMM) spores (10^7 spores/mL; Sanchez-Vallet et al., 2010) or spray-inoculated with flg22 (5 μM; Frerigmann et al., 2016). Leaf samples for quantitative analysis of IGs and their metabolism products in selected Arabidopsis genotypes were collected 16 h postinoculation with *B. graminis* conidiospores, 48 h after inoculation with *P. cucumerina* conidiospores, or 24 h after flg22 treatment and extracted in dimethyl sulfoxide as described by Bednarek et al. (2009). Extracts were subjected to HPLC on an Agilent 1200 HPLC System equipped with diode array and fluorescence detectors. Samples were analyzed on an Atlantis T3 C18 column (150 3 2.1 mm, 3 mm; Waters) according to the same protocols as reported earlier (Bednarek et al., 2009; Lu et al., 2015)

Disease Resistance Analyses

Erysiphe pisi

Arabidopsis (*Arabidopsis thaliana* and *A. lyrata*) plants were inoculated with conidiospores of *E. pisi* (Birmingham Isolate) using a settling tower (Lipka et al., 2005). Leaves were fixed, cleared, entry rates were scored, and secondary hyphae were visualized, as described earlier (Lipka et al., 2005).

Colletotrichum gloeosporioides

To investigate the trail of *C. gloeosporioides* and the development of primary biotrophic hyphae, 2 μL drops of *C. gloeosporioides* conidial suspension (approximately 5×10^5 conidia per mL) were drop-inoculated with 0.06% (w/v) Glc onto the cotyledon of each 12-d-old plant, and the inoculated plants were subjected to microscopic analysis at 14 h postinoculation. The method to count the types of *C. gloeosporioides* entry was described in Hiruma et al. (2010). To investigate the expansion of necrotrophic hyphae at the postentry and post-invasive defense stages, 5 μL drops of *C. gloeosporioides* conidial suspension (approximately 5×10^5 conidia per mL) were inoculated with 0.1% (w/v) Glc onto each of the leaves of 4-week-old plants. After incubation, the inoculated plants were subjected to lesion development analysis and Trypan Blue staining.

Plectospaerella cucumerina

Three-week-old Arabidopsis plants grown as previously described (Sanchez-Vallet et al., 2010) were inoculated with a spore suspension (4×10^6 spores/mL) of the adapted *P. cucumerina* BMM isolate (Ramos et al., 2013). Disease progression in the inoculated plants was estimated by determination of fungal DNA by means of qRT-PCR as described (Sánchez-Rodríguez et al., 2009). The qRT-PCR results are mean values $\pm$ SD from two technical replicates. At least three independent experiments ($n > 10$) were performed that gave similar results.

Callose Deposition Assay

Callose deposition in response to flg22 has been tested as described previously using 10-d-old Arabidopsis seedlings (Fukunaga et al., 2017). Treated seedlings were stained with Aniline Blue solution containing 0.005% Aniline Blue (Sigma-Aldrich) in 0.07 M sodium P buffer (pH 9) for 30 min (Adam and Somerville, 1996). The stained leaves were mounted on a slide in 50% glycerol and examined with a DAPI filter on an Olympus BX53 fluorescence microscope equipped with an Olympus DP72 camera and the Olympus cellSens program.

Comprehensive Targeted Coexpressions Analysis

Coexpression analysis was performed essentially as described previously (Nakano et al., 2017) using R software (http://www.r-project.org). CYPs, BGLUs, and GSTs were retrieved from The Arabidopsis Information Resources using PFAM annotation IDs (350 genes). To incorporate multiple genes assigned to single probes due to cross hybridization, probewise MR matrix was used as a distance matrix (311 probes). Coexpressed gene clusters were objectively determined by silhouette analysis. A table of genes and probes used in the analysis with the results from hierarchical clustering can be found in Supplemental Data S1. All scripts used for the analysis are available at http://www.mpipz.mpg.de/R_scripts.

Phylogenetic Analysis of GSTs

GSTs encoded on genome sequences of *A. lyrata*, *A. thaliana*, *Boechera stricta*, *Brassica rapa* FPsc, *Capsella grandiflora*, *Capsella rubella*, *Carica papaya*, *Chlamydomonas reinhardtii*, *Eutrema salsugineum*, *Gossypium raimondii*, *Manihot esculenta*, *Medicago truncatula* (v3.1 early release), *Oryza sativa*, *Physcomitrella patens*, *Selaginella moellendorffii*, *Sorghum bicolor*, *Theobroma cacao*, and *Volvox carteri* were collected from the Phytozome database (v.12) using the KEGG annotation term 2.5.1.18'. Resulting 1551 sequences were filtered based on sequence length (Supplemental Fig. S5), followed by multiple alignment using Muscle algorithm on MEGA7 software (http://www.megasoftware.net/). Out of 1073 sequences aligned, 325 gappy sequences were excluded by the MaxAlign on-line tool (http://www.cbs.dtu.dk/services/MaxAlign/) to ensure sufficient number of common sites. Aligned 748 sequences were subjected to ML analysis using the RAxML on-line tool (http://embnet.vital-it.ch/raxml-bb/), applying the GTR+G+I model. Bootstrap values were estimated by 100$\times$ replications. Phylogenetic trees were visualized using the iTOL on-line tool (http://itol.embl.de/). A list of genes that was included and excluded can be found in Supplemental Data S2.

Supplemental Data

The following supplemental materials are available.

Supplemental Figure S1. Silhouette analysis from coexpression matrix of *GSTs*, *CYPs*, and *BGLUs*.

Supplemental Figure S2. SALK_022297 and SALK_050148 lines are deficient in *GSTU13* transcript.

Supplemental Figure S3. GSH is required for the formation of 4OGlcI3F.

Supplemental Figure S4. Accumulation of I3A is induced in *gstu13* plants after flg22 treatment.

Supplemental Figure S5. Size-based filter of GSTs for phylogenetic analysis.

Supplemental Figure S6. ML tree of GSTs with full information.

Supplemental Data S1. Coexpression clustering table of GSTs, BGLUs, and CYPs, associated with Figure 2.

Supplemental Data S2. A summary table of genes used for the phylogenetic analysis, associated with Figure 7.

LITERATURE CITED

Adam L, Somerville SC (1996) Genetic characterization of five powdery mildew disease resistance loci in *Arabidopsis thaliana*. Plant J **9**: 341–356

Agerbirk N, De Vos M, Kim JH, Jander G (2009) Indole glucosinolate breakdown and its biological effects. Phytochem Rev **8**: 101–120

Alfenito MR, Souer E, Goodman CD, Buell R, Mol J, Koes R, Walbot V (1998) Functional complementation of anthocyanin sequestration in the vacuole by widely divergent glutathione *S*-transferases. Plant Cell **10**: 1135–1149

Bednarek P (2012a) Chemical warfare or modulators of defence responses—the function of secondary metabolites in plant immunity. Curr Opin Plant Biol **15**: 407–414

Bednarek P (2012b) Sulfur-containing secondary metabolites from *Arabidopsis thaliana* and other Brassicaceae with function in plant immunity. ChemBioChem **13**: 1846–1859

Bednarek P, Pislewska-Bednarek M, Svatos A, Schneider B, Doubsky J, Mansurova M, Humphry M, Consonni C, Panstruga R, Sanchez-Vallet A, Molina A, Schulze-Lefert P (2009) A glucosinolate metabolism pathway in living plant cells mediates broad-spectrum antifungal defense. Science **323**: 101–106

Bednarek P, Piślewska-Bednarek M, Ver Loren van Themaat E, Maddula RK, Svatoš A, Schulze-Lefert P (2011) Conservation and clade-specific

diversification of pathogen-inducible tryptophan and indole glucosinolate metabolism in *Arabidopsis thaliana* relatives. New Phytol 192: 713–726

Böttcher C, Westphal L, Schmotz C, Prade E, Scheel D, Glawischnig E (2009) The multifunctional enzyme CYP71B15 (PHYTOALEXIN DEFICIENT3) converts cysteine-indole-3-acetonitrile to camalexin in the indole-3-acetonitrile metabolic network of *Arabidopsis thaliana*. Plant Cell 21: 1830–1845

Clay NK, Adio AM, Denoux C, Jander G, Ausubel FM (2009) Glucosinolate metabolites required for an *Arabidopsis* innate immune response. Science 323: 95–101

Dixon DP, Edwards R (2010) Glutathione transferases. *In* The Arabidopsis Book. org/10.1199/tab.0131

Dixon DP, Hawkins T, Hussey PJ, Edwards R (2009) Enzyme activities and subcellular localization of members of the Arabidopsis glutathione transferase superfamily. J Exp Bot 60: 1207–1218

Dixon DP, Skipsey M, Edwards R (2010) Roles for glutathione transferases in plant secondary metabolism. Phytochemistry 71: 338–350

Francisco RM, Regalado A, Ageorges A, Burla BJ, Bassin B, Eisenach C, Zarrouk O, Vialet S, Marlin T, Chaves MM, Martinoia E, Nagy R (2013) ABCC1, an ATP binding cassette protein from grape berry, transports anthocyanidin 3-*O*-Glucosides. Plant Cell 25: 1840–1854

Frerigmann H, Piślewska-Bednarek M, Sánchez-Vallet A, Molina A, Glawischnig E, Gigolashvili T, Bednarek P (2016) Regulation of pathogen-triggered tryptophan metabolism in *Arabidopsis thaliana* by MYB transcription factors and indole glucosinolate conversion products. Mol Plant 9: 682–695

Fuchs R, Kopischke M, Klapprodt C, Hause G, Meyer AJ, Schwarzländer M, Fricker MD, Lipka V (2016) Immobilized subpopulations of leaf epidermal mitochondria mediate PENETRATION2-dependent pathogen entry control in Arabidopsis. Plant Cell 28: 130–145

Fukunaga S, Sogame M, Hata M, Singkaravanit-Ogawa S, Piślewska-Bednarek M, Onozawa-Komori M, Nishiuchi T, Hiruma K, Saitoh H, Terauchi R, Kitakura S, Inoue Y, et al (2017) Dysfunction of Arabidopsis MACPF domain protein activates programmed cell death via tryptophan metabolism in MAMP-triggered immunity. Plant J 89: 381–393

Geu-Flores F, Møldrup ME, Böttcher C, Olsen CE, Scheel D, Halkier BA (2011) Cytosolic γ-glutamyl peptidases process glutathione conjugates in the biosynthesis of glucosinolates and camalexin in Arabidopsis. Plant Cell 23: 2456–2469

Halkier BA, Gershenzon J (2006) Biology and biochemistry of glucosinolates. Annu Rev Plant Biol 57: 303–333

Hirai MY, Klein M, Fujikawa Y, Yano M, Goodenowe DB, Yamazaki Y, Kanaya S, Nakamura Y, Kitayama M, Suzuki H, Sakurai N, Shibata D, et al (2005) Elucidation of gene-to-gene and metabolite-to-gene networks in Arabidopsis by integration of metabolomics and transcriptomics. J Biol Chem 280: 25590–25595

Hiruma K, Fukunaga S, Bednarek P, Piślewska-Bednarek M, Watanabe S, Narusaka Y, Shirasu K, Takano Y (2013) Glutathione and tryptophan metabolism are required for Arabidopsis immunity during the hypersensitive response to hemibiotrophs. Proc Natl Acad Sci USA 110: 9589–9594

Hiruma K, Onozawa-Komori M, Takahashi F, Asakura M, Bednarek P, Okuno T, Schulze-Lefert P, Takano Y (2010) Entry mode-dependent function of an indole glucosinolate pathway in Arabidopsis for nonhost resistance against anthracnose pathogens. Plant Cell 22: 2429–2443

Hopkins RJ, van Dam NM, van Loon JJA (2009) Role of glucosinolates in insect-plant relationships and multitrophic interactions. Annu Rev Entomol 54: 57–83

Jacobs AK, Lipka V, Burton RA, Panstruga R, Strizhov N, Schulze-Lefert P, Fincher GB (2003) An Arabidopsis callose synthase, GSL5, is required for wound and papillary callose formation. Plant Cell 15: 2503–2513

Kim JH, Lee BW, Schroeder FC, Jander G (2008) Identification of indole glucosinolate breakdown products with antifeedant effects on *Myzus persicae* (green peach aphid). Plant J 54: 1015–1026

Kitamura S, Shikazono N, Tanaka A (2004) TRANSPARENT TESTA19 is involved in the accumulation of both anthocyanins and proanthocyanidins in Arabidopsis. Plant J 37: 104–114

Klein AP, Sattely ES (2017) Biosynthesis of cabbage phytoalexins from indole glucosinolate. Proc Natl Acad Sci USA 114: 1910–1915

Kolm RH, Danielson UH, Zhang Y, Talalay P, Mannervik B (1995) Isothiocyanates as substrates for human glutathione transferases: structure-activity studies. Biochem J 311: 453–459

Krajewski MP, Kanawati B, Fekete A, Kowalski N, Schmitt-Kopplin P, Grill E (2013) Analysis of Arabidopsis glutathione-transferases in yeast. Phytochemistry 91: 198–207

Kühnlenz T, Westphal L, Schmidt H, Scheel D, Clemens S (2015) Expression of *Caenorhabditis elegans* PCS in the *At*PCS1-deficient *Arabidopsis thaliana* cad1-3 mutant separates the metal tolerance and non-host resistance functions of phytochelatin synthases. Plant Cell Environ 38: 2239–2247

Labrou NE, Papageorgiou AC, Pavli O, Flemetakis E (2015) Plant GSTome: structure and functional role in xenome network and plant stress response. Curr Opin Biotechnol 32: 186–194

Lipka V, Dittgen J, Bednarek P, Bhat R, Wiermer M, Stein M, Landtag J, Brandt W, Rosahl S, Scheel D, Llorente F, Molina A, et al (2005) Pre- and postinvasion defenses both contribute to nonhost resistance in Arabidopsis. Science 310: 1180–1183

Lu X, Dittgen J, Piślewska-Bednarek M, Molina A, Schneider B, Svatoš A, Doubský J, Schneeberger K, Weigel D, Bednarek P, Schulze-Lefert P (2015) Mutant allele-specific uncoupling of PENETRATION3 functions reveals engagement of the ATP-Binding Cassette transporter in distinct tryptophan metabolic pathways. Plant Physiol 168: 814–827

Maeda K, Houjyou Y, Komatsu T, Hori H, Kodaira T, Ishikawa A (2009) AGB1 and PMR5 contribute to PEN2-mediated preinvasion resistance to *Magnaporthe oryzae* in *Arabidopsis thaliana*. Mol Plant Microbe Interact 22: 1331–1340

Marrs KA, Alfenito MR, Lloyd AM, Walbot V (1995) A glutathione S-transferase involved in vacuolar transfer encoded by the maize gene *Bronze-2*. Nature 375: 397–400

Mikkelsen MD, Buron LD, Salomonsen B, Olsen CE, Hansen BG, Mortensen UH, Halkier BA (2012) Microbial production of indolylglucosinolate through engineering of a multi-gene pathway in a versatile yeast expression platform. Metab Eng 14: 104–111

Mikkelsen MD, Olsen CE, Halkier BA (2010) Production of the cancer-preventive glucoraphanin in tobacco. Mol Plant 3: 751–759

Møldrup ME, Salomonsen B, Geu-Flores F, Olsen CE, Halkier BA (2013) De novo genetic engineering of the camalexin biosynthetic pathway. J Biotechnol 167: 296–301

Mueller LA, Goodman CD, Silady RA, Walbot V (2000) AN9, a petunia glutathione S-transferase required for anthocyanin sequestration, is a flavonoid-binding protein. Plant Physiol 123: 1561–1570

Nakano RT, Piślewska-Bednarek M, Yamada K, Edger PP, Miyahara M, Kondo M, Böttcher C, Mori M, Nishimura M, Schulze-Lefert P, Hara-Nishimura I, Bednarek P (2017) PYK10 myrosinase reveals a functional coordination between endoplasmic reticulum bodies and glucosinolates in *Arabidopsis thaliana*. Plant J 89: 204–220

Nishimura MT, Stein M, Hou B-H, Vogel JP, Edwards H, Somerville SC (2003) Loss of a callose synthase results in salicylic acid-dependent disease resistance. Science 301: 969–972

Obayashi T, Kinoshita K (2009) Rank of correlation coefficient as a comparable measure for biological significance of gene coexpression. DNA Res 16: 249–260

Parisy V, Poinssot B, Owsianowski L, Buchala A, Glazebrook J, Mauch F (2007) Identification of PAD2 as a γ-glutamylcysteine synthetase highlights the importance of glutathione in disease resistance of Arabidopsis. Plant J 49: 159–172

Pastorczyk M, Bednarek P (2016) Chapter Seven: The function of glucosinolates and related metabolites in plant innate immunity. *In* Kopriva S, ed, Glucosinolates, Vol 80, Academic Press/Elsevier, Cambridge, MA, pp 171–198

Pedras MSC, Yaya EE, Glawischnig E (2011) The phytoalexins from cultivated and wild crucifers: chemistry and biology. Nat Prod Rep 28: 1381–1405

Ramos B, González-Melendi P, Sánchez-Vallet A, Sánchez-Rodríguez C, López G, Molina A (2013) Functional genomics tools to decipher the pathogenicity mechanisms of the necrotrophic fungus *Plectosphaerella cucumerina* in *Arabidopsis thaliana*. Mol Plant Pathol 14: 44–57

Sánchez-Rodríguez C, Estévez JM, Llorente F, Hernández-Blanco C, Jordá L, Pagán I, Berrocal M, Marco Y, Somerville S, Molina A (2009) The ERECTA Receptor-Like Kinase regulates cell wall-mediated resistance to pathogens in *Arabidopsis thaliana*. Mol Plant Microbe Interact 22: 953–963

Sanchez-Vallet A, Ramos B, Bednarek P, López G, Piślewska-Bednarek M, Schulze-Lefert P, Molina A (2010) Tryptophan-derived secondary metabolites in *Arabidopsis thaliana* confer non-host resistance to necrotrophic *Plectosphaerella cucumerina* fungi. Plant J 63: 115–127

Schlaeppi K, Bodenhausen N, Buchala A, Mauch F, Reymond P (2008) The glutathione-deficient mutant *pad2-1* accumulates lower amounts of glucosinolates and is more susceptible to the insect herbivore *Spodoptera littoralis*. Plant J **55:** 774–786

Su T, Xu J, Li Y, Lei L, Zhao L, Yang H, Feng J, Liu G, Ren D (2011) Glutathione-indole-3-acetonitrile is required for camalexin biosynthesis in *Arabidopsis thaliana*. Plant Cell **23:** 364–380

Sun Y, Li H, Huang J-R (2012) Arabidopsis TT19 functions as a carrier to transport anthocyanin from the cytosol to tonoplasts. Mol Plant **5:** 387–400

Wagner U, Edwards R, Dixon DP, Mauch F (2002) Probing the diversity of the Arabidopsis glutathione *S*-transferase gene family. Plant Mol Biol **49:** 515–532

Wentzell AM, Rowe HC, Hansen BG, Ticconi C, Halkier BA, Kliebenstein DJ (2007) Linking metabolic QTLs with network and cis-eQTLs controlling biosynthetic pathways. PLoS Genet **3:** 1687–1701

Wittstock U, Kurzbach E, Herfurth AM, Stauber EJ (2016) Glucosinolate breakdown. *In* Kopriva S, ed, Glucosylates, **Vol. 80**. Academic Press/Elsevier, Cambridge, MA, pp 125–169

Zhang Y, Kolm RH, Mannervik B, Talalay P (1995) Reversible conjugation of isothiocyanates with glutathione catalyzed by human glutathione transferases. Biochem Biophys Res Commun **206:** 748–755

Zhou H, Jian R, Kang J, Huang X, Li Y, Zhuang C, Yang F, Zhang L, Fan X, Wu T, Wu X (2010) Anti-inflammatory effects of caper (*Capparis spinosa* L.) fruit aqueous extract and the isolation of main phytochemicals. J Agric Food Chem **58:** 12717–12721